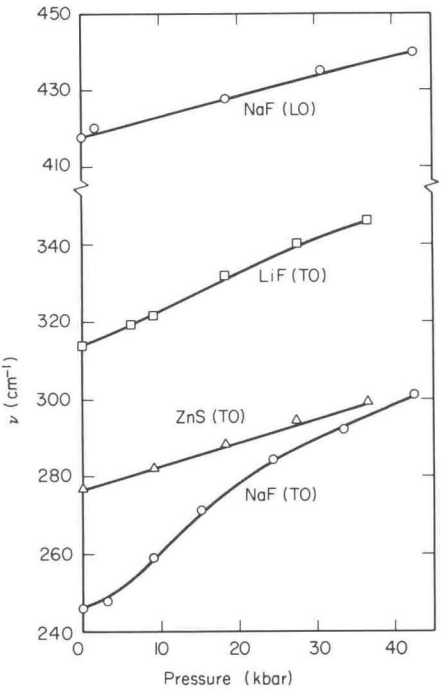

FIG. 1. Pressure dependences of several lattice vibrations.

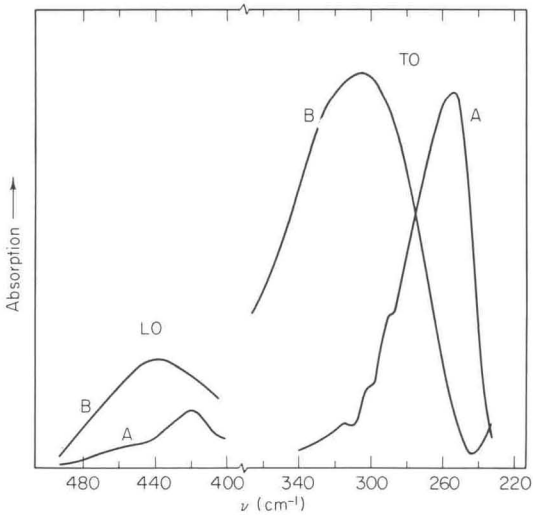

FIG 2. Comparison of the transverse and longitudinal modes in NaF with and without pressure.

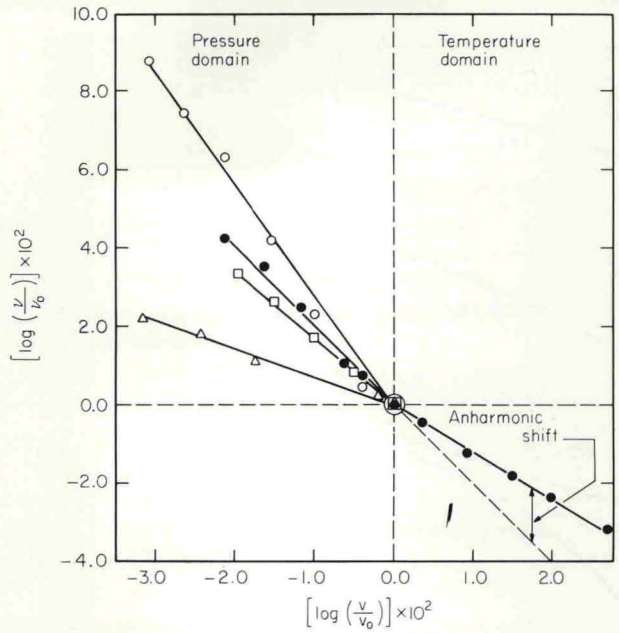

FIG. 3. Plot of ln ν/ν_0 vs. ln v/v_0 for several optic modes: (●) LiF (TO); (○) NaF (TO); (△) NaF (LO); (□) ZnS (TO).

observed that the straight line extrapolated from the pressure domain does not coincide with the line obtained from the temperature data. The difference may be attributed to the anharmonic contribution to the frequency shift (known as the "self-energy" shift), which increases steadily with increasing temperature of LiF. A similar analysis was made for KBr and in this crystal the "self-energy" shift is negligible. Results obtained for RbI using other techniques (*30*, *34*) also indicated negligible "self-energy" shifts.

The results obtained for the Grüneisen parameters for the long-wavelength optical modes from Eqs. (1) and (2),

$$\gamma_{j(k)} = -\partial \ln \nu_j(k)/\partial \ln V, \tag{2}$$

are given in Table IV. The agreement with the calculations made from those assuming a rigid-ion model with central forces incorporating repulsion terms of the Born–Mayer [$\exp(-r/p)$] and inverse-power (r^{-n}) type agree well. The results using Cowley's theory give somewhat larger values of γ.

The pressure dependences of two phases of a solid can be determined by these techniques (*31*). Such studies have been made with KBr (*31*) and KCl (*9*, *31*). Figure 4 shows the TO mode of KCl as a function of pressure. The difficulty of studying phase transitions is illustrated by the figures. The pressure gradient across the diamond anvils prevents the detection of a sharp